ELSEVIER

Biochimica et Biophysica Acta 1468 (2000) 187–198

BIOCHIMICA ET BIOPHYSICA ACTA
BBA

www.elsevier.com/locate/bba

A solid-state NMR study of the phospholamban transmembrane domain: local structure and interactions with Ca^{2+}-ATPase

Zareen Ahmed [a], David G. Reid [b], Anthony Watts [a], David A. Middleton [a,*]

[a] *Biomembrane Structure Unit, Department of Biochemistry, University of Oxford, South Parks Road, Oxford OX1 3QU, UK*
[b] *Safety Assessment Department, SmithKline Beecham Pharmaceuticals, The Frythe, Welwyn, Herts AL6 9AR, UK*

Received 8 March 2000; received in revised form 5 June 2000; accepted 7 June 2000

Abstract

The structure and dynamics of a double ^{13}C-labelled 24-residue synthetic peptide ($[^{13}C_2]CAPLB_{29-52}$), corresponding to the membrane-spanning sequence of phospholamban (PLB), were examined using ^{13}C cross-polarisation magic-angle spinning (CP-MAS) NMR spectroscopy. CP-MAS spectra of $[^{13}C_2]CAPLB_{29-52}$ reconstituted into unsaturated lipid membranes indicated that the peptide was mobile at temperatures down to −50°C. The NMR spectra showed that peptide motion became constrained in the presence of the SERCA1 isoform of Ca^{2+}-ATPase, and chemical cross-linking experiments indicated that $[^{13}C_2]CAPLB_{29-52}$ and Ca^{2+}-ATPase came into close contact with one another. These results together suggested that the peptide and the 110-kDa calcium pump were interacting in the membrane. Rotational resonance CP-MAS ^{13}C–^{13}C distance measurements on $[^{13}C_2]CAPLB_{29-52}$ reconstituted into lipid bilayers confirmed that the sequence spanning Phe-32 and Ala-36 was α-helical, and that this structure was not disrupted by interaction with Ca^{2+}-ATPase. These results support the finding that the transmembrane domain of PLB is partially responsible for regulation of Ca^{2+} transport through interactions with cardiac muscle Ca^{2+}-ATPase in the lipid bilayer, and also demonstrate the feasibility of performing structural measurements on PLB peptides when bound to their physiological target.

Keywords: Phospholamban; Magic angle spinning; Rotational resonance; Sarco(endo)plasmic reticulum Ca^{2+}-ATPase

1. Introduction

Phospholamban (PLB), a 52-residue membrane-spanning protein located almost exclusively in the sarcoplasmic reticulum (SR) of cardiac muscle, is the major target for phosphorylation by cAMP-dependent and calcium/calmodulin-dependent protein kinases in response to β-adrenergic stimulation [1]. PLB readily self-associates in lipid bilayers to form a 30-kDa homopentamer, which has been shown to function as a Ca^{2+} channel in reconstituted lipid bilayers [2]. The primary physiological role of PLB, however, is to regulate the active transport of calcium ions into the SR lumen through what is probably an inhibitory association of monomeric PLB with the SERCA2 isoform of Ca^{2+}-ATPase [3–5], which is

Abbreviations: NMR, nuclear magnetic resonance; MAS, magic-angle spinning; CP, cross polarization; PLB, phospholamban; SR, sarcoplasmic reticulum; SERCA, sarco(endo)plasmic reticulum Ca^{2+}-ATPase; DOPC, dioleoylphosphatidylcholine; DMPC, dimyristoylphosphatidylcholine; EDAC, 1-ethyl-3-(dimethylaminopropyl) carbodiimide; CD, circular dichroism

* Corresponding author. Fax: +44-1865-275234;
E-mail: middleda@bioch.ox.ac.uk

0005-2736/00/$ – see front matter
PII: S0005-2736(00)00257-1

reversed after phosphorylation of PLB at Ser-16 and Thr-17 [6,7].

Two structural domains of PLB have been proposed (Fig. 1). The first domain is a hydrophilic N-terminal sequence (residues 1–30) that extends from the membrane into the cytosol and contains the phosphorylation sites. Solution NMR data of PLB_{1-36} has shown that it consists of two predominantly α-helical stretches connected by a turn (residues Ile-18, Glu-19, Met-20 and Pro-21) that lies adjacent to the two phosphorylation sites [8]. The hydrophobic C-terminal sequence (residues 31–52) spanning the membrane bilayer constitutes the second domain. Studies of the membrane-spanning domain reconstituted into lipid bilayers, by circular dichroism [9] and Fourier transform infrared (FTIR) spectroscopy [10], both indicate a high degree of α-helical content, but are unable to define precise regions of α-helical structure.

The highest (2.6 Å) resolution structure of skeletal muscle Ca^{2+}-ATPase to date [11] has failed to shed light on possible sites of interaction with PLB, and the mechanism of Ca^{2+}-ATPase regulation remains unclear. Site-directed mutagenesis and functional studies have shown that the inhibitory association of PLB with Ca^{2+}-ATPase involves interactions with PLB not only in the cytoplasmic domain [12–14], but also within the transmembrane region [12,15]. Although the structure and activity of the cytoplasmic domain of PLB, and their response to phosphorylation, have been the subject of a number of studies, comparatively little is known about the details, and physiological importance, of Ca^{2+}-ATPase regulation by the PLB membrane domain.

Here, solid-state NMR was used to investigate the interaction between the membrane domain of PLB and Ca^{2+}-ATPase in reconstituted lipid bilayers to gain further insight into the mechanism of Ca^{2+} transport regulation. The high-resolution solid-state NMR technique of cross-polarisation magic-angle spinning (CP-MAS) NMR has emerged as a powerful tool for determining structural details of integral membrane proteins and peptides in intact lipid bilayers [16,17]. Here, a 23-residue ^{13}C-labelled peptide corresponding to the C-terminal domain of PLB ($[^{13}C_2]CAPLB_{29-52}$) was incorporated into phospholipid bilayers and its structure and dynamics were

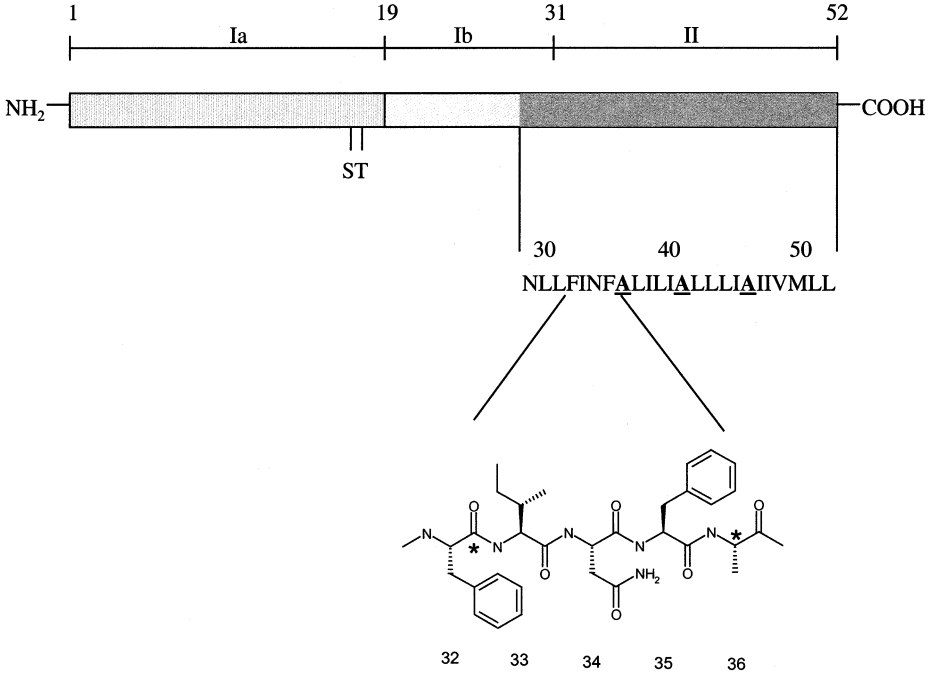

Fig. 1. Schematic diagram of phospholamban (PLB) showing the location of the *N*-terminal cytoplasmic domain (Ia, Ib) and the *C*-terminal membrane domain (II). The peptide $[^{13}C_2]CAPLB_{29-52}$ corresponds to the primary sequence of PLB shown from Asn-29 to Leu-52, and the expanded chemical structure of residues 32–36 show the sites of ^{13}C isotope labelling at the amide carbonyl of Phe-32 and the α-carbon of Ala-36. The underlined alanine residues were substituted in place of the three native cysteines of phospholamban.

examined using ^{13}C-CP-MAS NMR. The peptide was synthesised containing two ^{13}C-enrichment sites placed four residues apart (Fig. 1), and experiments were carried out [17–19] to qualitatively examine the peptide dynamics and to determine its local secondary structure in membranes containing the SERCA1 isoform of Ca^{2+}-ATPase from rabbit skeletal muscle sarcoplasmic reticulum.

2. Materials and methods

All reagents were from Sigma and of the highest grade available unless stated otherwise.

2.1. Peptide synthesis

[$^{13}C_2$]CAPLB$_{29-52}$ was prepared by solid-phase peptide synthesis from fmoc-protected amino acids (Dr. R. Shama and Prof. A. Lee, Southampton University) and purified by HPLC. The 24-amino acid peptide contained two ^{13}C-isotope labels at the carbonyl of Phe-32 and the Cα carbon of Ala-36 (Fig. 1). The three native cysteines were replaced by alanine to reduce the tendency of the peptide to self-associate [3,20,21] without changing its predicted secondary structural characteristics [22].

2.2. Characterisation and reconstitution of [$^{13}C_2$]CAPLB$_{29-52}$

The oligomeric state of the peptide in 2% SDS was characterised by SDS–polyacrylamide gel electrophoresis using a 10–20% gradient Tris-trycine gel. The gel was stained with SYPRO orange [23] and visualised under UV light at 300 nm.

Incorporation of [$^{13}C_2$]CAPLB$_{29-52}$ into synthetic phospholipid membranes was achieved by dissolving [$^{13}C_2$]CAPLB$_{29-52}$ (5 mg) with dimyristoylphosphatidylcholine (DMPC) or dioleoylphosphatidylcholine (DOPC) in $CHCl_3$:CH_3OH (5 ml) at a lipid-to-peptide molar ratio of 20:1 and drying to a thin film under vacuum. The film was rehydrated with phosphate buffer (5 ml, 10 mM KH_2PO_4, 50 mM NaCl, pH 7.0), vortexed and briefly sonicated in a water bath. The sample was then applied to a continuous sucrose gradient (5–25% w/w) and centrifuged overnight (120 000 × g at 4°C). The peptide-enriched membrane band was collected (at 20% sucrose concentration) and diluted in phosphate buffer for centrifugation (200 000 × g, 45 min, 4°C). The pellet was stored at −20°C.

2.3. Purification and functional characterisation of Ca^{2+}-ATPase

SERCA1 Ca^{2+}-ATPase was prepared from fast-twitch rabbit skeletal muscle sarcoplasmic reticulum according to the method of East and Lee [24]. The protein was characterised by SDS–polyacrylamide gel electrophoresis. Gels of 5% stacking and 10% resolving were electrophoresed and stained with Coomassie blue. Measurement of Ca^{2+}-ATPase hydrolytic activity was based on the methods of Hardwicke and Green [25], in which the rate of *p*-nitrophenyl phosphate hydrolysis was followed spectrophotometrically at 400 nm at 37°C for 5–10 min, using between 16.14 and 807 μg of protein.

2.4. Co-reconstitution of [$^{13}C_2$]CAPLB$_{29-52}$ and Ca^{2+}-ATPase

Co-reconstitution of [$^{13}C_2$]CAPLB$_{29-52}$ and Ca^{2+}-ATPase was carried out by dissolving the peptide (5 mg) and DOPC (28 mg) at a lipid-to-peptide molar ratio of 20:1, in $CHCl_3$:CH_3OH (5 ml) and drying to a thin film under vacuum. The film was rehydrated in phosphate buffer (1 ml) containing 12 mg/ml of sodium cholate detergent, which solubilises the Ca^{2+}-ATPase, vortexed and briefly sonicated in a water bath. Ca^{2+}-ATPase (25 mg) in a small volume of phosphate buffer (25 μl) was then added to the peptide suspension at a protein to peptide molar ratio of 1:8, and left for 15 min at room temperature and for 45 min at 4°C to equilibrate. After this time, the detergent was diluted to below its critical micelle concentration by addition of ice-cold phosphate buffer and centrifuged (200 000 × g, 45 min, 4°C). The resulting pellet was rehomogenised and suspended in phosphate buffer for centrifugation (200 000 × g, 45 min, 4°C). The pellet was stored at −20°C.

2.5. Chemical cross-linking

Experiments to cross-link [$^{13}C_2$]CAPLB$_{29-52}$ to Ca^{2+}-ATPase were carried out using a carbodiimide

coupling reagent 1-ethyl-3-(3-dimethylaminopropyl) (EDAC) [26]. A sample of co-reconstituted peptide and Ca^{2+}-ATPase in membranes was resuspended in phosphate buffer (1 ml) and the pH adjusted to 5.0 with HCl (0.1 M). EDAC was added with stirring to molar excess (5 mg) and left for 60 min on ice. The pH was then adjusted to pH 7.0 with NaOH (0.1 M) and allowed to continue stirring for 60 min on ice and then for a further 60 min at room temperature. The sample was then centrifuged (200 000 × *g*, 45 min, 4°C) to a pellet.

2.6. Circular dichroism spectroscopy

Three samples were prepared for CD spectroscopy (alongside peptide-free samples): (1) [$^{13}C_2$]-CAPLB$_{29-52}$ (100 μg) solubilised in 2% SDS (in phosphate buffer) to a final peptide concentration of 3 μM; (2) [$^{13}C_2$]CAPLB$_{29-52}$ (160 μg) reconstituted in DMPC (1.98 mg) at a lipid-to-peptide molar ratio of 50:1, to a final peptide concentration of 29 μM in phosphate buffer; and (3) [$^{13}C_2$]CAPLB$_{29-52}$ reconstituted in DMPC and resolubilised in β-octylglucoside (10 mM, in phosphate buffer) to a final peptide concentration of 15 μM.

CD measurements were carried out on a JASCO J720 spectropolarimeter. All spectra were recorded at room temperature over a wavelength of 195 to 250 nm. The path length of the quartz cell was 1 mm. All spectra were corrected by subtracting the peptide free sample. Results are expressed in terms of ellipticity in units of deg cm^2 dmol^{-1}.

2.7. NMR spectroscopy

All ^{13}C-MAS NMR spectra were acquired on a modified Bruker AMX360WB spectrometer at a magnetic field of 8.3 T, using a standard Bruker double-resonance 4-mm magic-angle spinning probe tuned to the ^{13}C and ^{1}H Larmor frequencies. For low temperature experiments, the pre-dried bearing gas was passed through a heat exchanger immersed in liquid nitrogen before connection to the probe. Samples were packed into zirconia rotors fitted with boron nitride caps and rotated at the magic-angle at spinning frequencies ($\omega_r/2\pi$) of up to 11 000 Hz.

Magnetisation exchange experiments were carried out at the $n = 1$ ($\omega_r/2\pi = 10950$ Hz) and $n = 2$ ($\omega_r/2\pi = 5545$ Hz) rotational resonance condition. Hartmann–Hahn cross-polarisation (CP) from ^{1}H to ^{13}C was achieved at a nutation frequency of 60 kHz over a dipolar contact time of 1.6 ms, immediately followed by a ^{13}C-flip-back 90° pulse (4 μs). The peptide ^{13}Cα-spins were selectively inverted using a DANTE pulse train and detected after incremented mixing intervals (0.1–60 ms) that allow exchange of Zeeman order between the two ^{13}C-spins. ^{13}C-Magnetisation was returned to the transverse plane by applying another non-selective 4-μs 90° pulse, and the signal was digitally sampled into 1 K complex data points. Protons were decoupled at a field of 83 kHz from immediately after CP until each transient had been collected [27]. The sample spinning speed was kept constant (within 5 Hz) and the temperature maintained at −50°C. FIDs were Fourier transformed into 4K of data points after applying 20 Hz of exponential line broadening.

3. Results

3.1. Protein reconstitution

Methods were used to prepare phospholipid bilayers containing a homogeneous distribution of [$^{13}C_2$]CAPLB$_{29-52}$ and Ca^{2+}-ATPase. The hydrophobic peptide was readily incorporated into DOPC and DMPC bilayers after co-dissolution (lipid-to-peptide molar ratio of 20:1) in organic solvents. Purification was carried out by density gradient centrifugation of the membranes, which gave a single narrow band that sedimented separately from lipid-only dispersions. SDS–polyacrylamide gel electrophoresis of peptide-containing membranes exhibited a single band under fluorescent light after SYPRO Orange staining, corresponding to a molecular weight range of 2–5 kDa (densitometric scans of the gels are shown Fig. 2). Protein staining was absent from higher molecular weight regions of the gel suggesting that the three Cys–Ala substitutions prevented the peptide from self-associating in SDS micelles. The monomeric state of the peptide was anticipated from the results of previous site-directed mutagenesis studies [3,20,21], but recent evidence for oligomerisation of a similar peptide sequence

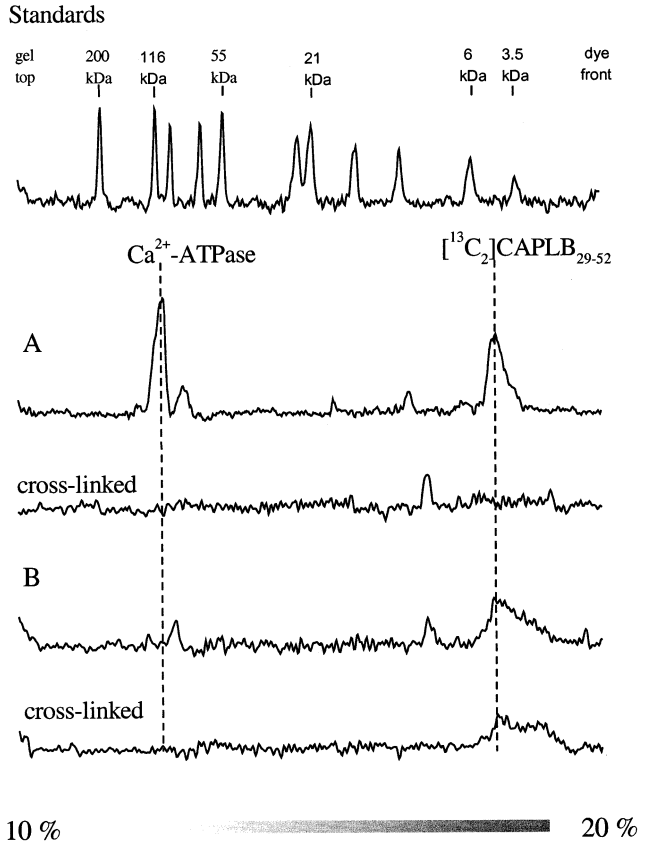

Fig. 2. Densitometric scans of SYPRO Orange-stained SDS–PAGE gels (10–20% polyacrylamide gradient) of $[^{13}C_2]$-$CAPLB_{29-52}$ in DOPC membranes. Samples contained lipid, peptide and Ca^{2+}-ATPase in a molar ratio of 160:8:1 (A) or lipid and peptide only, in a molar ratio of 20:1 (B). Membrane samples were solubilised in SDS and electrophoresed without boiling (A and B, top scans), or first incubated for 3 h with the cross-linking reagent EDAC (A and B, bottom scans).

to $[^{13}C_2]CAPLB_{29-52}$ has been found independently by gel electrophoresis [28].

$[^{13}C_2]CAPLB_{29-52}$ was co-reconstituted with Ca^{2+}-ATPase from cholate detergent into DOPC membranes to a final peptide-to-protein molar ratio of 8:1 and a peptide to lipid molar ratio of 1:20. The maximal hydrolytic activity (V_{max}) of Ca^{2+}-ATPase was 19.1 μmol/mg/min in the native SR preparation, but fell to 6.0 μmol/mg/min in pure DOPC membranes, and lower still to 2.4 μmol/mg/min in membranes containing the peptide (Table 1). It is known that reconstitution of Ca^{2+}-ATPase using cholate detergent results in a partial loss of ATP hydrolysis [29–30], but the further loss of activity seen in the presence of $[^{13}C_2]CAPLB_{29-52}$ conflicts with the results of previous work showing that the transmembrane domain of PLB reduces only the affinity of Ca^{2+}-ATPase for Ca^{2+} without affecting the rate of ATP hydrolysis [12]. SDS–PAGE gels of the membrane exhibited major bands from Ca^{2+}-ATPase and $[^{13}C_2]CAPLB_{29-52}$ centred approximately at 110 and 3 kDa, respectively, as well as a small number of less prominent peaks corresponding to protein impurities in the SR membrane preparation (Fig. 2).

Chemical cross-linking studies formed the basis for the initial hypothesis that the physiological role of PLB involves direct interaction of its cytoplasmic domain with Ca^{2+}-ATPase [7]. Here, the chemical cross-linking agent EDAC was used to determine whether $[^{13}C_2]CAPLB_{29-52}$ and Ca^{2+}-ATPase could come into close enough contact with each other in the membrane to support an inhibitory interaction [12,15]. EDAC links a primary amine to a carboxyl group (and to a lesser extent, cysteine sulfhydryl and tyrosine aryl hydroxyl groups) through a short spac-

Table 1
Summary of the structural and functional data obtained for $[^{13}C_2]CAPLB_{29-52}$ (lipid-to-peptide molar ratio of 20:1) and rabbit skeletal muscle Ca^{2+}-ATPase in lipid bilayers and native membranes

Protein sample	Lipid membrane	V_{max} (μmol/mg/min)	$F_{32}INFA_{36}$ distance (Å)[a]	
			$n=1$	$n=2$
$[^{13}C_2]CAPLC_{29-52}$	DMPC	–	4.3 ± 0.3	4.9 ± 0.9
$[^{13}C_2]CAPLB_{29-52}$+Ca^{2+}-ATPase[b]	DOPC	2.40	5.3 ± 0.3	5.2 ± 0.8
	DOPC (cross-linked)	0.05	–	5.2 ± 1.7
Ca^{2+}-ATPase	Native	19.1	–	–
	DOPC	6.00	–	–

[a]Distance measurements ($^{13}C\alpha$–^{13}CO) were carried out at $n=1$ and $n=2$ rotational resonance.
[b]The peptide-to-protein molar ratio was 8:1.

ing sequence, provided the reactive side-groups lie adjacent to each other. The N-terminally acetylated [$^{13}C_2$]CAPLB$_{29-52}$ has a single free carboxyl group at the C-terminus, but no primary amines, and therefore cannot couple to other peptide molecules in the membrane. Hence, the peptide C-terminus presents a unique site in [$^{13}C_2$]CAPLB$_{29-52}$ for reaction with EDAC, whereas Ca^{2+}-ATPase has a preponderance of lysine ε-amino groups with the potential for cross-linking to the peptide.

Densitometric scans of SDS–PAGE gels of peptide-containing membranes after incubation with EDAC for 3 h are shown in Fig. 2. Gels of [$^{13}C_2$]CAPLB$_{29-52}$ membranes exhibited a single diffuse band of similar intensity and molecular weight range before and after incubation with EDAC, but when the peptide was co-reconstituted with Ca^{2+}-ATPase and incubated with EDAC the 110 and 3 kDa bands disappeared from the SDS–PAGE gel. Since [$^{13}C_2$]CAPLB$_{29-52}$ is unable to cross-link to itself, it was assumed that all of the peptide had coupled to Ca^{2+}-ATPase to form high molecular weight conjugates that are unable to enter the gel. Hydrolytic activity of Ca^{2+}-ATPase was lost almost entirely after cross-linking with the peptide (Table 1).

3.2. Dynamics of reconstituted [$^{13}C_2$]CAPLB$_{29-52}$

It was possible to rule out the existence of a separate fraction of peptide-containing membranes from which Ca^{2+}-ATPase was excluded, because all of the peptide was able to cross-link to Ca^{2+}-ATPase. More crucially, the results indicated that the peptide and Ca^{2+}-ATPase were able to interact closely with each other in the membrane. It was not known, however, if the lifetime of the interaction was long enough to be physiologically important, or whether the proteins were coupled together by EDAC simply because of random molecular collisions resulting from lateral diffusion in the membrane.

NMR experiments were carried out to examine more closely the nature of the interaction between Ca^{2+}-ATPase and [$^{13}C_2$]CAPLB$_{29-52}$, by qualitative investigation of peptide dynamics. Membrane peptides can undergo several modes of motion, including rotational diffusion and lateral diffusion within the plane of the bilayer, with rates depending on the membrane environment [31,32]. The rates of peptide rotational and lateral diffusion are generally highest for small peptides sequences in fluid lipid bilayers, but can be reduced considerably in the event of constraining interactions with other proteins or interactions between extramembranous regions of the peptide and the lipid headgroups. Hence, a study of the dynamics of the peptide in reconstituted membranes might provide some information on the equilibrium state of the molecular interactions taking place between [$^{13}C_2$]CAPLB$_{29-52}$ and Ca^{2+}-ATPase.

The ^{13}C-NMR signal intensity from membrane proteins and peptides under CP-MAS conditions has been found to diminish in the presence of molecular motion [33]. Peptide dynamics may give rise to slow rates of cross-polarisation from ^{1}H to ^{13}C, shorter $T_{1\rho}$ relaxation times or interference with proton decoupling, each of which can lead to a reduction in signal intensity. Hence, it is usually desirable to freeze out peptide motions in order to maximise signal intensity [17]. Here, however, the potentially destructive effects of molecular dynamics on the CP-MAS spectrum were used to qualitatively assess the comparative dynamics of [$^{13}C_2$]CAPLB$_{29-52}$ in different environments and in the presence of Ca^{2+}-ATPase.

Proton-decoupled ^{13}C-CP-MAS NMR experiments were performed on the peptide incorporated into DMPC and DOPC bilayers with and without Ca^{2+}-ATPase. Peaks from Ala-36 (^{13}Cα) at 54 ppm and Phe-32 (^{13}CO) at 177 ppm are clearly visible in spectra of the reconstituted peptide (Fig. 3). The ^{13}Cα-resonance of [$^{13}C_2$]CAPLB$_{29-52}$ is complicated by the fact that it has a similar chemical shift to the natural abundance —CH_3 resonance from the choline lipid head group ($\sim$54ppm). To avoid interference from the choline signal, the peptide was therefore reconstituted into headgroup-deuterated lipids for all quantitative NMR experiments. The choline resonance is not observed in ^{13}C CP-MAS NMR spectra of d_9-DOPC and d_9-DMPC because of the absence of local protons to transfer polarisation to the methyl carbon nuclei. Spectra of [$^{13}C_2$]-CAPLB$_{29-52}$ co-reconstituted into DOPC bilayers with Ca^{2+}-ATPase contained additional contributions from the natural abundance resonances of the protein, but the two peptide resonances at 54 and 177 ppm remained clearly visible and provided an essential peptide signature that enabled [$^{13}C_2$]-

$CAPLB_{29-52}$ to be observed in the mixed protein bilayer (Fig. 3).

Spectra of the peptide in the different membrane preparations were recorded over temperatures ranging from −10 to −60°C. Peptide signal intensity profiles over the temperature range were plotted from the integrals of the peptide carbonyl peak at 177 ppm. In all cases, the peptide peak intensities diminished as the temperature was raised from −60 to −10°C, probably because of increasing mobility of the peptides as the membranes grew more fluid at higher temperatures (Fig. 4). Fully membrane-embedded peptides such as gramicidin also show rapid rotational diffusion in fluid membranes [34] while peptides with hydrophilic sequences extending beyond the lipid bilayer, such as the M13 coat-protein, are motionally restrained even in fluid lipid membranes (Dr. C. Glaubitz, personal communication).

The peaks from the peptide in pure DOPC bilayers disappeared at temperatures of −20°C and above, while a rather less pronounced decline in intensity was observed from peptide when incorporated into DMPC bilayers (Fig. 4). Unsaturated and saturated lipid bilayers differ quite markedly in fluidity over the experimental temperature range; pure DOPC undergoes chain melting at about −22°C while DMPC remains well ordered throughout (DMPC phase transition +23°C). Hence, it is expected that the mobility of the peptide would be rather more constrained in the DMPC bilayers than in the more fluid DOPC bilayers, and the CP-MAS intensity profiles are consistent with this prediction. When $[^{13}C_2]CAPLB_{29-52}$ was incorporated into DOPC membranes containing Ca^{2+}-ATPase, the decline in signal intensity was unlike that of the peptide in pure DOPC bilayers, but instead was rather similar to that from the peptide in DMPC membranes (Fig. 4). This finding suggests that the mobility of the peptide becomes more constrained in DOPC membranes when Ca^{2+}-ATPase is also present. Such motional constraints are unlikely to arise from the self-association of $[^{13}C_2]CAPLB_{29-52}$, since this would be ex-

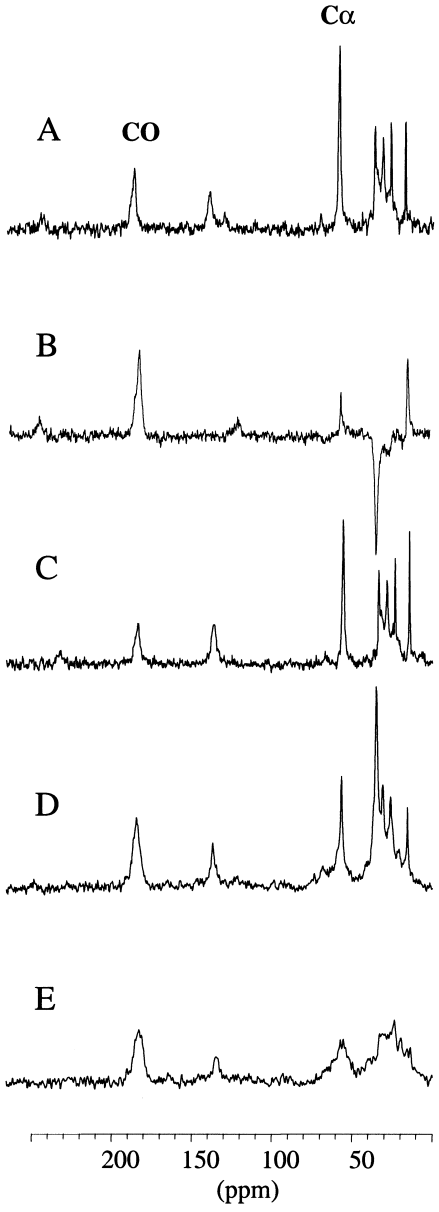

←

Fig. 3. Proton decoupled ^{13}C-CP-MAS NMR spectra of membranes containing $[^{13}C_2]CAPLB_{29-52}$, Ca^{2+}-ATPase or both. The protein and peptide were reconstituted into headgroup-deuterated d_9-DOPC membranes (A–D) in a lipid-to-peptide molar ratio of 20:1 and spectra were obtained from the following peptide-to-protein molar ratios: (A) $[^{13}C_2]CAPLB_{29-52}$ only; (B) $[^{13}C_2]CAPLB_{29-52}$ with polarisation inversion; (C) $[^{13}C_2]$-$CAPLB_{29-52}$ and Ca^{2+}-ATPase at a 20:1 molar ratio; (D) $[^{13}C_2]CAPLB_{29-52}$ and Ca^{2+}-ATPase at an 8:1 molar ratio; (E) Ca^{2+}-ATPase in native SR membranes. Reconstituted samples contained 5 mg of peptide, and SR membrane samples contained 10 mg protein. In the polarisation inversion spectrum, the resonances from the lipid hydrocarbon CH_2 groups have negative intensity, the CH resonances from peptide α-carbons are suppressed and resonances from the DOPC headgroup (arrowed) and hydrocarbon terminal CH_3 groups remain positive. The MAS frequency was 5 kHz in all experiments.

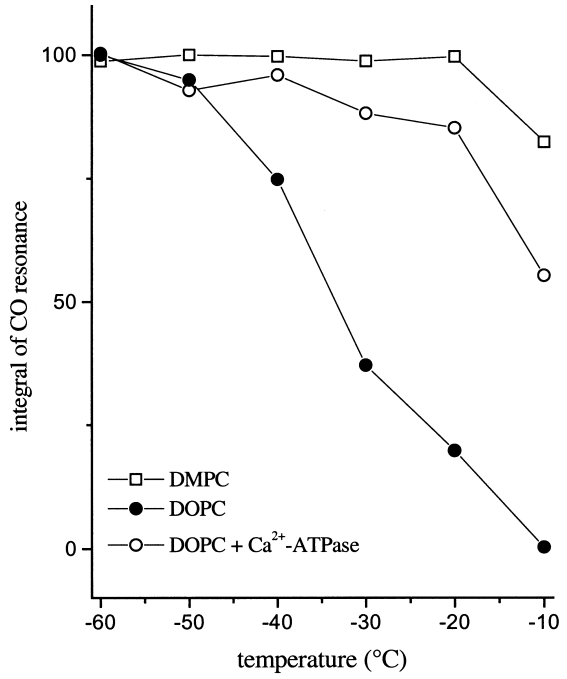

Fig. 4. The temperature dependence of ^{13}C-CP-MAS NMR spectra of [$^{13}C_2$]CAPLB$_{29-52}$ in lipid membranes containing DOPC, DMPC and DOPC with Ca^{2+}-ATPase. The data points show the integral of the carbonyl resonance from ^{13}C-labelled Phe-32 over a temperature range of 50°C. The lipid-to-peptide molar ratio was 20:1, and the peptide-to-protein molar ratio was 8:1.

pected to occur with equal probability in the absence of Ca^{2+}-ATPase, and it is more probable that it is interactions of the peptide with the much larger calcium pump that are responsible for the reduced peptide mobility.

Hence, the cross-linking experiments indicated that the protein and peptide are able to come into close contact, and NMR indicated that the lifetime of the interaction was long on the NMR time-scale.

3.3. *Conformational studies of CAPLB$_{29-52}$ using circular dichroism*

Circular dichroism (CD) was used to examine the secondary structural content of [$^{13}C_2$]CAPLB$_{29-52}$ in a membrane-simulating environment. Spectra indicated that the peptide adopts a mostly α-helical conformation in an aqueous solution of 2% SDS, as characterised by the presence of the large minimum in the CD spectrum at 208 nm and 222 nm (Fig. 5). The spectrum of [$^{13}C_2$]CAPLB$_{29-52}$ reconstituted in DMPC at a lipid-to-peptide molar ratio of 50:1 also shows minima at 208 and 222 nm, signifying a α-helical structure in the presence of lipid. Solubilised complexes of the DMPC membranes containing [$^{13}C_2$]CAPLB$_{29-52}$ with β-octylglucoside (0.34 M), produced a CD signal comparable to that observed with [$^{13}C_2$]CAPLB$_{29-52}$ in 2% SDS. The secondary structure of the peptide in the presence of Ca^{2+}-ATPase could not be examined because of the overwhelming contribution from the ion-pump to the spectrum, which could not be deconvoluted from the relatively minor component from the peptide.

Quantification of individual secondary structural contributions to the spectra was not made because interpretation of CD spectra of membrane proteins may not be straightforward owing to the presence of artefacts arising from scattering effects [35,36]. Qualitative analysis of the spectrum by visual inspection shows the peptide exists largely in a α-helical conformation in the environments examined, as observed for other similar peptide fragments of PLB [20].

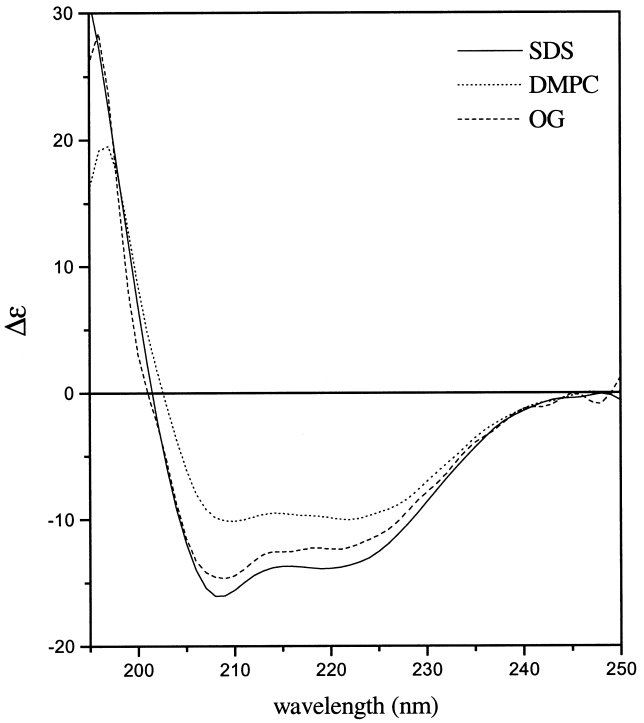

Fig. 5. Circular dichroic spectra of [$^{13}C_2$]CAPLB$_{29-52}$. Spectra are shown for the peptide solubilised in 2% SDS (solid line), incorporated in DMPC membranes to a lipid-to-peptide ratio of 50:1 (dotted line) and resolubilised from the membranes in β-octyl glucoside (dashed line). Spectra are shown in elipticity units ($\times 10^{-3}$ deg cm^2 dmol^{-1}).

3.4. Structure of reconstituted $[^{13}C_2]CAPLB_{29-52}$ using NMR

The CD spectra agreed with previous studies [9] and indicated that the transmembrane domain of PLB adopts a largely α-helical structure in detergent micelles and phospholipid membranes, but gave no impression of which regions of the peptide, if any, are helical and which are not. Moreover, CD is unable to provide qualitative indications of the peptide secondary structure in the presence of Ca^{2+}-ATPase because of interference from the protein. CP-MAS NMR was therefore used to examine the secondary structure in the transmembrane domain in greater detail, and also to examine how, if at all, the structure is affected by the presence of Ca^{2+}-ATPase.

Rotational resonance, a method based on CP-MAS NMR, was used to confirm the local secondary structure of $[^{13}C_2]CAPLB_{29-52}$ over a region spanning five residues (Phe-32–Ile-33–Asn-34–Phe-35–Ala36) putatively lying close to the membrane–water interface, by measuring the through-space distance between the ^{13}C sites placed four residues apart (Fig. 1). Distances are determined in the rotational resonance experiment by measuring weak homonuclear dipole couplings (between ^{13}C and ^{13}C, for example), which are introduced when the sample spinning frequency (ν_r) is equal to (or is a sub-multiple of) the frequency separating the isotropic chemical shifts ($\Delta\nu_{IS}$) of the nuclei [27]. Under rotational resonance, an experiment is performed to measure the rate of magnetisation exchange between the nuclei by measuring the signal intensities from the two nuclei over a series of mixing intervals. The magnetisation exchange rate is analysed to determine the dipolar coupling constant, which is inversely proportional to internuclear distance. Computer modelling of $[^{13}C_2]CAPLB_{29-52}$ in various secondary structures showed that the ^{13}C–^{13}C distance was diagnostic of secondary structure, and ranged from a maximum of 12.0 Å for a β-strand to a minimum of 5.1 Å for an α-helix. For pairs of ^{13}C-labels, measurable magnetisation exchange occurs when the nuclei are separated by up to 6.5 Å.

$[^{13}C_2]CAPLB_{29-52}$ was incorporated into pure DOPC bilayers and into DOPC membranes containing Ca^{2+}-ATPase to a peptide-to-protein molar ratio of 8:1, and magnetisation exchange experiments were carried out at first-order ($\nu_r = \Delta\nu_{IS}$) and second-order ($\nu_r = \Delta\nu_{IS}/2$) rotational resonance. The temperature was maintained at −50°C to reduce the residual rotational diffusion of the peptide, which might otherwise average the dipolar couplings measured. The differences in the peak intensities (after subtraction of natural abundance signal) for Phe-32 (CO) and Ala-36 (Cα) were measured at a number of mixing intervals and plotted in Fig. 6 to show the extent of magnetisation exchange at rotational resonance. In all experiments, magnetisation exchange was found to occur only at rotational resonance and not at sample spinning frequencies well away from rotational resonance, indicating that magnetisation is exchanged under the influence of ^{13}C–^{13}C coupling

Numerical simulations of the experimental magnetisation exchange data [27] were carried out to obtain values of the Phe-32 to Ala-36 ^{13}C–^{13}C distances in the two membrane samples. The rotational resonance magnetisation exchange profile is dependent not only on the distance-dependent dipole coupling constant d_{IS}, but also on the relative orientations of the chemical shielding tensors of the two spins and on a damping factor, the zero-quantum relaxation rate $1/T_2^{ZQ}$ [27]. The zero-quantum relaxation time T_2^{ZQ} can have a dominant effect on the exchange profile and is difficult to determine accurately, although an estimate can be obtained from the spectral line widths. Owing to these additional determinants of magnetisation decay and the uncertainties in their measurement, the experimental data was simulated by calculating a series of curves corresponding to many random combinations of d_{IS}, T_2^{ZQ} and the angles defining the chemical shift tensor orientations. The upper and lower limits of the ^{13}C–^{13}C interatomic distance were deduced from the computed curves falling within the upper and lower error limits of the experimental data (Fig. 6).

The ^{13}C–^{13}C distances measured for $[^{13}C_2]$-$CAPLB_{29-52}$ in the different membrane environments are summarised in Table 1. The distance ranged from 4.2 to 5.5 Å in the case of peptide incorporated into pure DOPC bilayers, and from 4.5 to 5.7 Å for the non-cross-linked peptide in membranes containing Ca^{2+}-ATPase. Models of the pentapeptide sequence in different secondary structures showed that the distances predicted for β-sheet (12.0 Å) and extended configuration (13.3 Å) structures were too long to

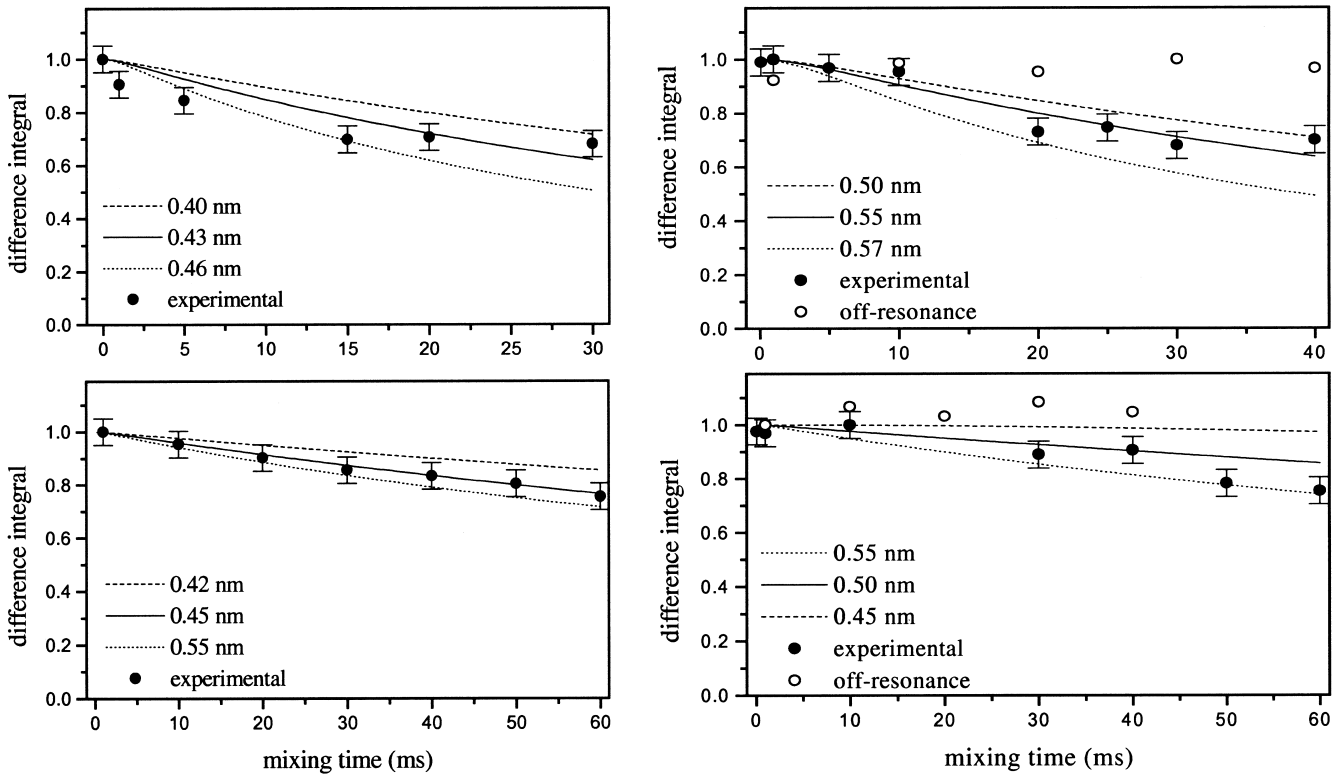

Fig. 6. Plots of magnetisation exchange (filled circles) for $[^{13}C_2]$CAPLB$_{29-52}$ at $n=1$ (top) and $n=2$ (bottom) rotational resonance at a constant temperature of −50°C. Data was obtained for $[^{13}C_2]$CAPLB$_{29-52}$ when reconstituted into pure DMPC bilayers (left graphs) to a lipid-to-peptide molar ratio of 20:1, and when co-reconstituted with Ca^{2+}-ATPase in DOPC bilayers (right graphs) to a lipid-to-peptide-to-protein ratio of 20:8:1. The error bars represent the signal-to-noise ratio in the spectra. Curves representing the upper-limit (dashed line), lower-limit (dotted line) and best-fit (solid line) to the experimental data were calculated as described in Section 3.4, and corresponded to the interatomic distances stated on each graph.

give rise to any measurable magnetisation decay and could be ruled out definitively. In fact, the distances determined by rotational resonance were consistent only with an α-helical structure across the pentapeptide region both when $[^{13}C_2]$CAPLB$_{29-52}$ is incorporated in pure lipid bilayers and when the peptide interacts with the membrane-exposed surface of Ca^{2+}-ATPase. Distance measurements also suggested that the pentapeptide region retained its α-helical structure after cross-linking of the peptide to Ca^{2+}-ATPase (Table 1).

4. Discussion

The peptide $[^{13}C_2]$CAPLB$_{29-52}$, which corresponds to the assumed monomeric [3,20,21] transmembrane domain of phospholamban, was here found to be α-helical in a pentapeptide region expected to lie close to the membrane–water interface. CD spectra of the peptide in detergent micelles provide evidence that much of transmembrane peptide is α-helical, which was also the finding of CD studies on similar peptide sequences [9]. Some uncertainty exists as to where in the transmembrane domain the helical structure is broken, and this work has reduced this uncertainty by pinpointing, for the first time, and with some certainty, a region of the peptide that is α-helical.

NMR and cross-linking studies indicate that an interaction takes place between reconstituted monomeric $[^{13}C_2]$CAPLB$_{29-52}$ and Ca^{2+}-ATPase in the membrane, which does not involve disruption of the peptide's helical structure in the region examined (Table 1). It is known that the interaction of the transmembrane domain of PLB with the cardiac (SERCA2a) isoform of Ca^{2+}-ATPase impedes protein function [15], but the structural features relating the molecular interaction to the inhibitory effect are

not clear. Our results show that the V_{max} of Ca^{2+}-ATPase hydrolytic activity is reduced in the presence of $[^{13}C_2]$CAPLB$_{29-52}$, while others have found that similar peptide fragments of PLB reduce only the affinity of the enzyme for calcium ions [12,15]. Since single mutations have been shown to alter the oligomeric state of PLB [3,37], it is also conceivable that subtle differences in the primary sequence of PLB in the membrane domain, such as the three Cys–Ala substitutions in $[^{13}C_2]$CAPLB$_{29-52}$, can cause the hydrolytic activity of Ca^{2+}-ATPase to be reduced [15] without affecting the affinity of the enzyme for calcium.

Cross-linking and mutagenesis studies have identified a peptide sequence in the acylphosphorylation region of Ca^{2+}-ATPase that may form the inhibitory site of interaction with the cytoplasmic domain of PLB [14]. Although water-soluble peptides corresponding to the cytoplasmic domain of PLB have shown some inhibitory activity against Ca^{2+}-ATPase [12], full regulation of the calcium pump can only occur when the transmembrane region of PLB is also present [38,39]. Here, EDAC cross-linking (Fig. 2) and variable temperature CP-MAS NMR spectra (Fig. 4) suggest that the α-helical transmembrane region of PLB binds to Ca^{2+}-ATPase even at a peptide concentration that is 8-fold higher than that of the protein.

The high level of binding of $[^{13}C_2]$CAPLB$_{29-52}$ to Ca^{2+}-ATPase raises questions about the specificity of the interaction compared with the proposed 1:1 interaction between full-length PLB and Ca^{2+}-ATPase. Non-specific interactions between the hydrophobic transmembrane domain of PLB and Ca^{2+}-ATPase may be minimised by the size of the 28-residue cytoplasmic domain, while no such steric barrier is present in $[^{13}C_2]$CAPLB$_{29-52}$. Nevertheless, it is likely that strong interactions within the membrane do occur between full-length PLB and Ca^{2+}-ATPase, and a model for the regulatory function of PLB should therefore take account of the balance between strong hydrophobic interactions within the membrane and electrostatic forces in the cytoplasm. Phosphorylation of PLB has been shown by fluorescence and NMR spectroscopy to be coupled to a conformational change in the cytoplasmic domain [40,41], and there is some evidence that the structural change in phosphorylated PLB may cause the monomers to dissociate from their inhibitory site and reform pentamers [42,43]. It is possible that conformational changes occurring after phosporylation of PLB create repulsive forces in the cytoplasm that counter the forces of attraction in the membrane.

Acknowledgements

We acknowledge the financial support of the BBSRC (Z.A. and A.W.) in collaboration with Smithkline Beecham Pharmaceuticals, and HEFCE. We would like to thank Dr. R. Shama and Professor A. Lee, University of Southampton, for synthesis and Dr. C. Glaubitz for assistance with data analysis.

References

[1] M. Tada, M. Inui, J. Mol. Cell. Cardiol. 15 (1983) 565–575.
[2] R.J. Kovacs, M.T. Nelson, H.K.B. Simmerman, L.R. Jones, J. Biol. Chem. 263 (1988) 18364–18368.
[3] Y. Kimura, K. Kurzydlowski, M. Tada, D.H. MacLennan, J. Biol. Chem. 272 (1997) 15061–15064.
[4] I.T. Arkin, P.D. Adams, A.T. Brunger, S. Aimoto, D.M. Engelman, S.O. Smith, J. Membr. Biol. 155 (1997) 199–206.
[5] D.L. Stokes, Curr. Opin. Struct. Biol. 4 (1994) 197–203.
[6] E.G. Kranias, J.L. Garvey, R.D. Srivastava, R.J. Solara, Biochem. J. 226 (1985) 113–121.
[7] P. James, M. Inui, M. Tada, M. Chiesi, E. Carafoli, Nature 342 (1989) 90–92.
[8] P. Pollesello, A. Annila, M. Ovaska, Biophys. J. 76 (1999) 1784–1795.
[9] I.T. Arkin, M. Rothman, C.F.C. Ludlam, S. Aimoto, D.M. Engelman, K.J. Rothschild, S.O. Smith, J. Mol. Biol. 248 (1995) 824–834.
[10] S.A. Tatulian, L.R. Jones, L.G. Reddy, D.L. Stokes, L.K. Tamm, Biochemistry 34 (1995) 4448–4456.
[11] C. Toyoshima, M. Nakasako, H. Nomura, H. Ogawa, Nature 405 (2000) 647–655.
[12] T. Sasaki, M. Inui, Y. Kimura, T. Kuzuya, M. Tada, J. Biol. Chem. 267 (1992) 1674–1679.
[13] G. Hughes, J.M. East, A.G. Lee, Biochem. J. 303 (1994) 511–516.
[14] T. Toyofuku, K. Kurzydlowski, M. Tada, D.H. MacLennan, J. Biol. Chem. 269 (1994) 3088–3094.
[15] Y. Kimura, K. Kazimierz, M. Tada, D.H. MacLennan, J. Biol. Chem. 271 (1996) 21726–21731.
[16] T.A. Cross, Curr. Opin. Struct. Biol. 4 (1994) 574–581.
[17] S.O. Smith, K. Aschheim, M. Groesbeek, Quart. Rev. Biophys. 29 (1996) 395–449.
[18] F.A. Creuzet, Science 251 (1990) 783–786.

[19] D.A. Middleton, R. Robins, X. Feng, M.H. Levitt, I.D. Spiers, C.H. Schwalbe, D.G. Reid, A. Watts, FEBS Lett. 410 (1997) 269–274.
[20] I.T. Arkin, EMBO J. 13 (1994) 4757–4764.
[21] H.K.B. Simmerman, Y.M. Kobayashi, J.M. Autry, L.R. Jones, J. Biol. Chem. 271 (1996) 5941–5946.
[22] P.Y. Chou, G.D. Fasman, Annu. Rev. Biochem. 47 (1978) 251–276.
[23] T.H. Steinberg, L.J. Jones, R.P. Haugland, V.L. Singer, Anal. Biochem. 239 (1996) 223–237.
[24] J.M. East, A.G. Lee, Biochemistry 21 (1982) 4144–4151.
[25] P.M.D. Hardwicke, N.M. Green, Eur. J. Biochem. 42 (1974) 183–193.
[26] S. Bauminger, M. Wilcheck, Methods Enzymol. 70 (1980) 151–159.
[27] M.H. Levitt, D.P. Raleigh, F. Creuzet, R.G. Griffin, J. Chem. Phys. 92 (1990) 6347–6364.
[28] C.G. Marquardt, G.W. Hunter, L.R. Jones, D.D. Thomas, C.B. Karim Biophys. J. 76 (1999) A122, Pos529.
[29] D.H. MacLennan, J. Biol. Chem. 245 (1970) 4508–4518.
[30] G. Hughes, A.P. Starling, R.P. Sharma, J.M. East, A.G. Lee, Biochem. J. 318 (1996) 973–979.
[31] P.F. Knowles, D. Marsh, Biochem. J. 274 (1991) 625–641.
[32] M.M. Sperotto, Eur. Biophys. J. 26 (1997) 405–416.
[33] D.E. Warschawski, J.D. Gross, R.G. Griffin, J. Chim. Phys. Phys.-Chim. Biol. 95 (1998) 460–466.
[34] R.S. Prosser, J.H. Davis, Biophys. J. 66 (1994) 1429–1440.
[35] R.W. Woody, Methods Enzymol. 246 (1995) 34–71.
[36] W.C. Johnson, Proteins Struct., Funct. Genet. 7 (1990) 205–214.
[37] L.G. Reddy, J.M. Autry, L.R. Jones, D.D. Thomas, J. Biol. Chem. 274 (1999) 7649–7655.
[38] L.G. Reddy, L.R. Jones, S.E. Cala, J.J. Orbrian, S.A. Tatulian, D.L. Stokes, J. Biol. Chem. 270 (1995) 9390–9397.
[39] L.R. Jones, L.J. Field, J. Biol. Chem. 268 (1993) 11486–11488.
[40] M. Li, R.L. Cornea, J.M. Autry, L.R. Jones, D.D. Thomas, Biochemistry 37 (1998) 7869–7877.
[41] R. Mortishire-Smith, S.M. Pitzenberger, C. Burke, C.R. Middaugh, V.M. Garsky, R.G. Johnson, Biochemistry 34 (1995) 7603–7613.
[42] R.L. Cornea, L.R. Jones, J.M. Autry, D.D. Thomas, Biochemistry 36 (1997) 2960–2967.
[43] H.K.B. Simmerman, L.R. Jones, Physiol. Rev. 78 (1998) 921–947.